

Structure of the N-WASP EVH1 Domain-WIP Complex: Insight into the Molecular Basis of Wiskott-Aldrich Syndrome

Brian F. Volkman,^{1,4} Kenneth E. Prehoda,^{2,4,5}
Jessica A. Scott,^{2,6} Francis C. Peterson,¹
and Wendell A. Lim^{2,3}

¹Department of Biochemistry
Medical College of Wisconsin
Milwaukee, Wisconsin 53226

²Department of Cellular and Molecular
Pharmacology
University of California, San Francisco
San Francisco, California 94143

Summary

Missense mutants that cause the immune disorder Wiskott-Aldrich Syndrome (WAS) map primarily to the Enabled/VASP homology 1 (EVH1) domain of the actin regulatory protein WASP. This domain has been implicated in both peptide and phospholipid binding. We show here that the N-WASP EVH1 domain does not bind phosphatidyl inositol-(4,5)-bisphosphate, as previously reported, but does specifically bind a 25 residue motif from the WASP Interacting Protein (WIP). The NMR structure of the complex reveals a novel recognition mechanism—the WIP ligand, which is far longer than canonical EVH1 ligands, wraps around the domain, contacting a narrow but extended surface. This recognition mechanism provides a basis for understanding the effects of mutations that cause WAS.

Introduction

Spatial and temporal regulation of the actin cytoskeleton is essential for controlling cell shape and movement. The Wiskott-Aldrich Syndrome Protein (WASP) and its homolog N-WASP are signal transduction proteins that have emerged as central players that promote actin polymerization in response to upstream intracellular signals (Carlier et al., 1999; Snapper and Rosen, 1999; Higgs and Pollard, 2001; Millard and Machesky, 2001; Pollard et al., 2000). Mutation of WASP, which is primarily expressed in hematopoietic cells, results in Wiskott-Aldrich Syndrome (WAS), an X-linked recessive disorder characterized by immunodeficiency, eczema, and thrombocytopenia (Derry et al., 1994; Kolluri et al., 1995; Villa et al., 1995; Greer et al., 1996; Zhu et al., 1997). These symptoms are consistent with cytoskeletal defects in hematopoietic cells (Zicha et al., 1998) and a possible role of WASP/N-WASP in motility, thrombogenesis, endocytosis, phagocytosis, and other actin-based processes (Snapper et al., 1998; Snapper and Rosen, 1999; Cannon et al., 2001; Coppolino et al., 2001; Le-

verrier et al., 2001). Similarly, a knockout mutation of the more ubiquitously expressed N-WASP gene results in embryonic lethality and defects in many but not all actin-based motility processes (Snapper et al., 2001). These proteins have also been hijacked by pathogens including shigella and vaccinia virus as required components for their own actin-based intracellular motility (Suzuki et al., 1998; Moreau et al., 2000).

Recent studies have begun to uncover the molecular mechanism by which WASP/N-WASP regulates actin polymerization. WASP and N-WASP have a highly modular domain structure (Figure 1A). A ~100 residue C-terminal “output” domain containing a verprolin-cofilin-acidic motif (VCA) directly binds to and activates the actin-related protein (Arp)2/3 actin nucleating complex (Machesky and Insall, 1998; Rohatgi et al., 1999), whereas the remaining regions of WASP/N-WASP, which encompass multiple domains, are involved in targeting and regulating the activity of the output domain in response to upstream signaling inputs. An important goal is to understand the function of the regulatory domains found in WASP/N-WASP in order to understand what signals regulate WASP and the mechanism of this regulation. Several of the domains, including the basic motif (B), the GTPase binding domain (GBD), and the proline-rich region, have been found to participate directly or indirectly in autoinhibitory interactions that repress or block the activity of the VCA output domain (Miki et al., 1998; Kim et al., 2000; Prehoda et al., 2000). These autoinhibitory interactions are specifically relieved by interaction with upstream activators including the phospholipid phosphatidyl inositol-(4,5)-bisphosphate (PIP₂), the GTPase Cdc42, and Src homology 3 (SH3) domain-containing proteins such as Nck (Higgs and Pollard, 2000; Prehoda et al., 2000; Rohatgi et al., 2000, 2001; Carlier et al., 2000).

One of the most important domains in WASP is the Enabled/VASP Homology 1 domain (also known as WASP Homology 1 or WH1 domain) located at the N terminus of the protein (Gertler et al., 1996; Symons et al., 1996; Callebaut et al., 1998; Renfranz and Beckerle, 2002). The functional importance of the WASP EVH1 domain is underscored by the fact that 28 of the 35 identified missense mutations that lead to the disease WAS are concentrated within this domain (Derry et al., 1995; El-Hakeh et al., 2002; Greer et al., 1996; Kolluri et al., 1995; Zhu et al., 1997). In addition, this domain is required for N-WASP-dependent intracellular motility of vaccinia virus (Moreau et al., 2000).

EVH1 domains are found in several other proteins, including the cytoskeletal regulatory proteins Enabled and VASP and the neuronal signaling protein Homer (Callebaut et al., 1998; Gertler et al., 1996). In these cases, the EVH1 domain appears to serve as a modular protein-peptide docking unit that can participate in protein targeting. These previously characterized EVH1 domains all utilize a conserved aromatic binding surface to recognize specific, 6–10 residue proline-rich peptide motifs (Prehoda et al., 1999; Fedorov et al., 1999; Carl et al., 1999; Ball et al., 2000; Beneken et al., 2000; Barzik

³Correspondence: wlim@itsa.ucsf.edu

⁴These authors contributed equally to this work.

⁵Present address: Institute of Molecular Biology, University of Oregon, Eugene, Oregon 97403.

⁶Present address: University of Wisconsin Medical School, Madison, Wisconsin 53706.

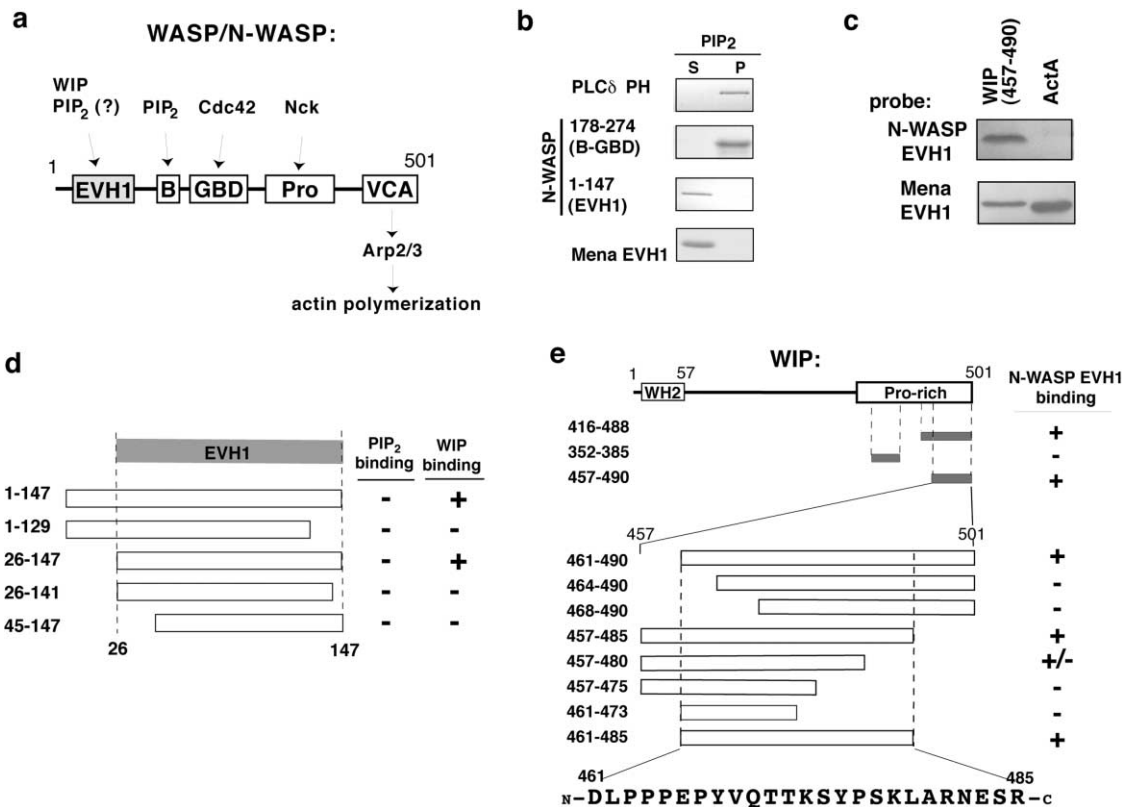


Figure 1. The N-Terminal Region of N-WASP Is an EVH1 Domain that Binds WIP via an Extended Peptide Ligand

(A) Proposed domain structure of N-WASP, as well as putative ligands for each domain.

(B) Example PIP₂ vesicle binding assays. S indicates supernatant, P indicates pellet. Bound protein is retained in the pellet. The PLCδ PH domain and the N-WASP EVH1 fragment were expressed as fusions to glutathione-S-transferase (GST). Remaining proteins were expressed as His₆-tag fusions.

(C) Example far-Western protein binding assays. Probe proteins were biotinylated by expressing them as fusions to the Promega Pinpoint vector (see Experimental Procedures). Each protein was tested for binding to a GST-fusion to WASP Interacting Protein (WIP) fragment containing residues 457–490 and to the ActA sequence DFPPPTDEEL, which is a ligand for the Mena EVH1 domain.

(D) Summary of PIP₂ and WIP (457–490) binding using various N-WASP constructs. None of the constructs bind PIP₂, but all those that precisely encompass the predicted EVH1 region can bind the WIP fragment.

(E) Deletion mapping reveals that a 25 residue polypeptide from WIP (residues 461–485) is the minimal fragment required for binding to the N-WASP EVH1 domain (residues 26–147) in a far-Western gel overlay binding assay.

et al., 2001). Thus, it has been postulated that the WASP/N-WASP EVH1 domain may also serve a targeting function.

Despite its importance in the pathology of WAS, the precise molecular function of the WASP EVH1 domain has remained unclear (Insall and Machesky, 1999). Several functions have been ascribed to the domain, including binding to the acidic phospholipid, phosphatidylinositol (4,5) bisphosphate (PIP₂) (Imai et al., 1999; Miki et al., 1996) and binding to the WASP interacting protein (WIP) (Ramesh et al., 1997), both of which are known regulators of N-WASP-mediated actin polymerization. EVH1 domains share the same overall fold with Pleckstrin Homology (PH) domains (Fedorov et al., 1999; Prehoda et al., 1999; Ball et al., 2000; Barzik et al., 2001; Beneken et al., 2000), many of which specifically bind phosphoinositides (Rebecchi and Scarlata, 1998). Thus, it has been suggested that EVH1 domains may be bifunctional, interacting with both peptides and phosphoinositides (Prehoda et al., 1999).

WIP is an actin binding protein that contains several

proline-rich sequences that may be putative EVH1 domain binding motifs (Martinez-Quiles et al., 2001; Moreau et al., 2000; Naqvi et al., 1998; Ramesh et al., 1997; Savoy et al., 2000). It has not been determined, however, if these motifs are sufficient to mediate the interaction between WASP and WIP. Furthermore, homology modeling based on known EVH1 domain structures fails to explain the behavior of several of the most common WAS-causing mutations—specifically, the most significant mutational hotspot associated with severe WAS is located at a surface that is predicted to lie directly opposite the canonical peptide binding surface (Beneken et al., 2000; Prehoda et al., 1999). These inconsistent findings have several possible explanations: (1) the N-WASP/WASP EVH1 domain may differ significantly in structure from other EVH1 domains; (2) these domains may have multiple binding sites—one that interacts with peptides and another that interacts with other ligands such as PIP₂; or (3) these domains may use a mechanism of peptide interaction that is significantly different from that of other EVH1 domains.

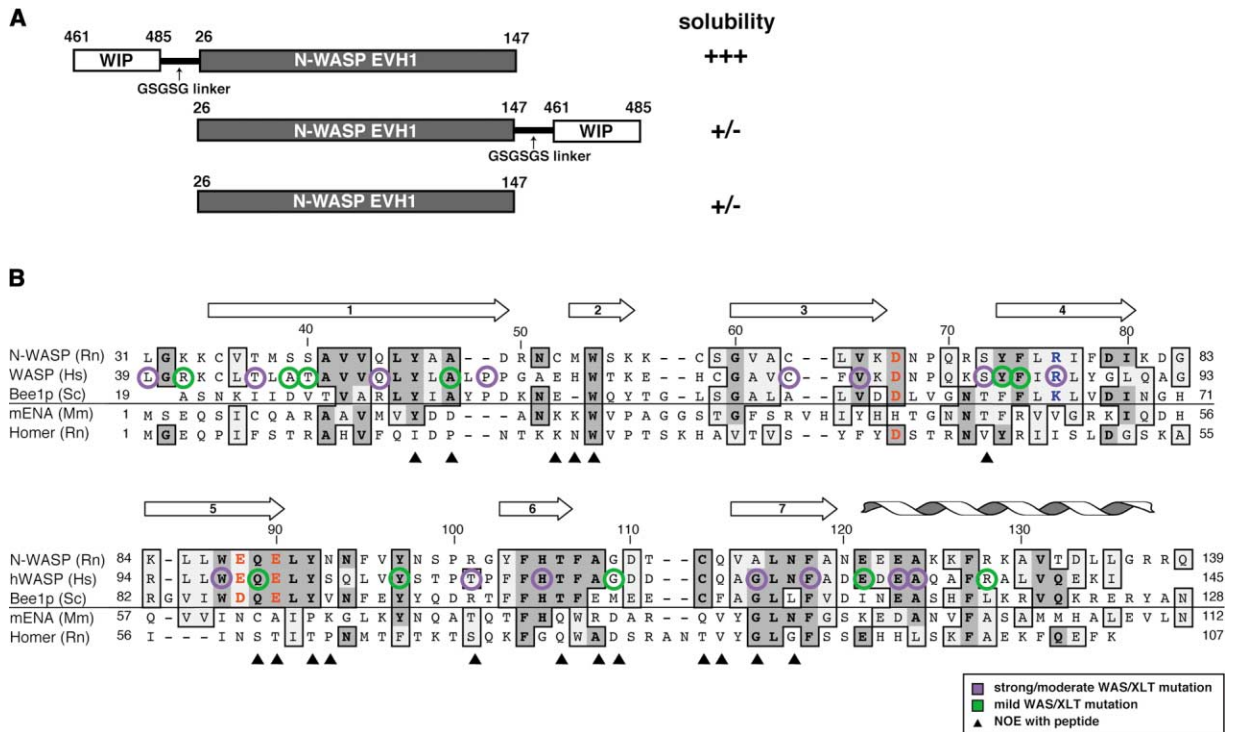


Figure 2. N-WASP EVH1 Domain Sequence

(A) Constructs of the N-WASP EVH1 domain fused to the minimal WIP peptide. Fusions are linked via a (Gly-Ser-Gly-Ser-Gly) linker. Only the top fusion yielded highly soluble protein amenable to structural analysis.

(B) Structure-based alignment of the Rat N-WASP EVH1 domain with its close homologs WASP (*H. sapiens*) and Bee1p (*S. cerevisiae*). Also shown are sequences of other more distantly related, but structurally characterized EVH1 domains. Secondary structure elements in the N-WASP structure are indicated above the sequence. Sites that show a direct NOE contact with the WIP peptide are marked by filled triangles. Sites in WASP where missense mutation cause the disease WAS are circled (lavender, strong/moderate phenotype; green, mild phenotype). A conserved charged residue array in the WASP family EVH1 domains, described in Figure 5, are indicated in red (negative) or blue (positive).

Here, we have sought to clarify what ligands the N-WASP EVH1 domain can specifically bind and how WAS-causing mutants may disrupt these interactions. We find that the N-WASP EVH1 domain and other EVH1 domains cannot bind PIP₂ with significant affinity, contrary to a previous report. However, we find that the N-WASP EVH1 domain can specifically interact with a 25 residue peptide from WIP. We have determined the structure of the EVH1-WIP peptide complex using NMR spectroscopy, revealing that the domain adopts the same overall fold as other EVH1 domains, but it utilizes a novel mechanism of peptide recognition. The WIP peptide, which is more than twice as long as typical EVH1 ligands, wraps around the entire EVH1 domain like a piece of string around a spool, contacting regions on the domain surface extending far beyond the canonical EVH1 peptide binding site. The structure reveals a novel class of domain-mediated protein-protein interactions and suggests how WAS-causing mutations are likely to disrupt the WASP/WIP interaction.

Results and Discussion

The EVH1 Domain of N-WASP Does Not Bind PIP₂

It was previously reported that the N-terminal region of N-WASP including the EVH1 domain was a PH or PH-like domain capable of PIP₂ binding (Miki et al., 1996). We

generated several fragments encompassing the mouse N-WASP EVH1 domain and tested them for phospholipid binding. Phospholipid vesicle binding assays show that none of the N-WASP fragments are capable of binding PIP₂ with detectable affinity using this assay (Figure 1B). In contrast, in the same assay, strong PIP₂ binding is observed for two other known lipid binding modules: the Pleckstrin Homology (PH) domain from phospholipase C-delta (PLC- δ) and a fragment of N-WASP (residues 178–274) that includes a highly basic region (B domain) that has recently been shown to mediate PIP₂ regulation in N-WASP (Prehoda et al., 2000; Rohatgi et al., 2001). We also show that a canonical EVH1 domain, from the protein Mena, is also not capable of binding PIP₂ in this assay. Thus, despite a high degree of structural homology with PH domains, EVH1 domains do not generally appear to share the function of high-affinity phosphoinositide binding, at least at a level comparable to that observed for canonical PH domains ($K_d \sim 1 \mu\text{M}$).

The Minimal EVH1 Ligand Is a 25 Residue Peptide from WIP

In contrast, in far-Western protein binding assays, we found that N-WASP fragments encompassing the EVH1 region were responsible for binding to a fragment from WIP (residues 416–488) that had previously been shown to interact with N-WASP (Figure 1C). The fragment of

N-WASP required for WIP binding correlates precisely with the EVH1 domain boundaries (Figure 1D).

The 72 residue WIP fragment contains many proline-rich putative EVH1 binding motifs, so we used deletion analysis to delineate the minimal recognition requirements (Figure 1E). A 25 amino acid fragment of WIP (residues 461–485) is minimally required for recognition. This motif is well conserved in certain isoforms of the recently identified WIP homolog CR16 (Ho et al., 2001) and the yeast homolog verprolin (Naqvi et al., 1998), and its presence appears to correlate with ability to bind N-WASP. The WIP motif encompasses a proline-rich motif (DLPPPEP) similar to that recognized by the EVH1 domain from Mena (DFPPPT). In our assays, the WIP sequence, in fact, crossreacts with the Mena EVH1 domain, although the N-WASP EVH1 domain does not crossreact with a 10 residue ligand for the Mena EVH1 domain from the protein ActA (Niebuhr et al., 1997; Prehoda et al., 1999).

The most striking feature of the minimal N-WASP EVH1 domain binding motif is that at 25 residues, it is more than twice as long as the minimal 6–10 residue peptides sufficient for Mena, VASP, or Homer EVH1 recognition (Niebuhr et al., 1997; Prehoda et al., 1999; Ball et al., 2000; Barzik et al., 2001; Beneken et al., 2000), suggesting that the binding energy is well-distributed across this motif. Interestingly, the isolated N-WASP EVH1 domain is highly insoluble and is poorly expressed, precluding any high-resolution structural or biochemical studies. However, we found that when we fused the 25 residue WIP motif to the N terminus of the EVH1 domain via a 5 residue linker, the protein now expressed extremely well in bacteria and was highly soluble (Figure 2A). In contrast, however, a similar fusion of the WIP peptide to the C terminus did not yield soluble protein, thereby indicating a dependence on stereochemical orientation.

Structure of the EVH1 Domain-WIP Peptide Complex: A Novel “Wrapping”

Mechanism of Recognition

The unusual length of the WIP polypeptide required for N-WASP EVH1 binding suggests a novel mechanism of interaction that could, for example, depend on higher-order secondary or tertiary structure of the ligand. To understand how the WIP polypeptide interacts with the N-WASP EVH1 domain, we determined the NMR structure of the highly soluble fusion protein encompassing the interaction pair described above (Table 1).

Structural analysis of the EVH1-WIP complex utilized the single-chain construct described above. However, to confirm that the covalent linker did not affect the mode of WIP binding, we also produced a second analogous construct with a thrombin cleavage site in the linker. After purification, this construct could be cleaved to completion and remained as a soluble complex. No differences were observed in backbone triple-resonance or NOESY NMR spectra acquired on samples of each version of the complex (cleaved or tethered), aside from new residues introduced in the thrombin recognition site (see Supplemental Figure S1 at <http://www.cell.com/cgi/content/full/111/4/565/DC1>), illustrating that the presence of a covalent link has no effect on WIP peptide binding mode.

Table 1. Structural Statistics for 20 WIP-EVH1 Structures

NOE Constraints	Number	
Long	803	
Medium	278	
Short	455	
Intraresidue	348	
Total ^a	1884	
WIP/EVH1 NOEs ^b	135	
Ramachandran Statistics ^c		
Most favored	76.4%	
Additionally allowed	20.7%	
Generously allowed	2.0%	
Disallowed	0.9%	
Parameter	Family	Minimized Average
Target function (Å ²)	0.86 ± 0.17	0.76
Upper limit violations		
Number > 0.1 Å	10 ± 3	4
Sum of violations (Å)	5.1 ± 0.7	3.8
Maximum violation (Å)	0.24 ± 0.07	0.19
Torsion angle violations		
Number > 5°	0 ± 0	0
Sum of violations (°)	0.4 ± 0.1	0.4
Maximum violation (°)	0.05 ± 0.01	0.03
Van der Waals violations		
Number > 0.2 Å	0 ± 1	0
Sum of violations (Å)	3.4 ± 0.5	3.9
Maximum violation (Å)	0.17 ± 0.07	0.16
Atomic Rmsds ^d (Å): Family of 20 Structures versus Mean		
Backbone	0.50 ± 0.06	
Heavy atom	0.94 ± 0.08	

^a Unique, nontrivial constraints derived from a total of 4305 NOEs observed in four separate 2D and 3D NOESY spectra using the CALIBA function of the DYANA program.

^b Constraints between residues of the WIP sequence and residues of the N-WASP EVH1 domain.

^c Only residues observed by NMR, corresponding to WIP residues 461–480 and N-WASP residues 34–137, were included in Ramachandran analysis.

^d Disordered linker and loop residues were excluded. Rmsd calculations included WIP residues 462–468 and 474–479

The overall fold of the N-WASP EVH1 domain is similar to that observed for the Mena, Homer, and VASP domains (Fedorov et al., 1999; Prehoda et al., 1999; Beneken et al., 2000; Barzik et al., 2001). The structure-based alignment of several EVH1 domain sequences is shown in Figure 2B.

The structure reveals, however, a novel mode of EVH1-mediated interaction—the WIP polypeptide exists in a largely extended conformation and wraps around much of the domain, like a piece of string around a concave spool (Figure 3A). Because of the extended nature of the ligand, the surface of the EVH1 domain that is contacted for recognition is far larger (~900 Å²) than the canonical binding surfaces utilized by the Mena and Homer EVH1 domains to recognize their much shorter peptide ligands (~300 Å²) (Figures 3B and 3C). Nonetheless, as a part of its interaction, the N-WASP EVH1 domain does use the conserved canonical binding surface to recognize a highly proline-rich portion of its cognate motif (discussed below).

The overall interaction of the N-WASP EVH1 domain with this extended WIP polypeptide has unexpected

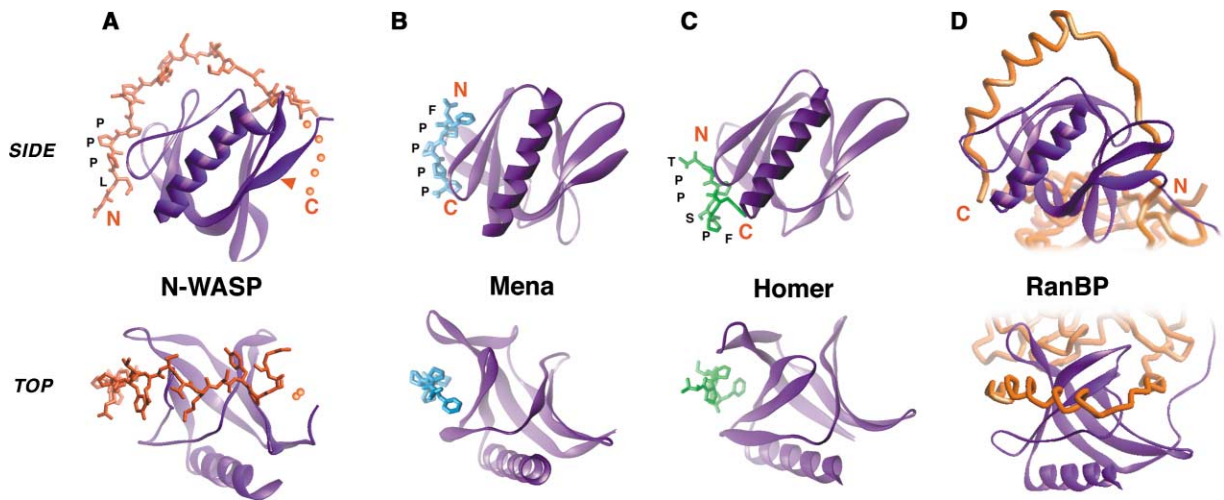


Figure 3. Structure of the N-WASP/WIP Complex Determined by NMR and Comparison to Other EVH1 Domain-Mediated Complexes
 (A) N-WASP EVH1 domain in complex with WIP residues 461–485. Note that residues 480–485 are required for binding but are poorly defined in the structure because of a lack of assignments and constraints. The likely path of those residues is indicated by the dotted line. The red arrow indicates the site of the most common severe WAS missense mutation, Arg76 [86]. This site falls at the opposite surface from the canonical EVH1 binding surface.
 (B) Structure of the Mena EVH1 domain in complex with an 8 residue peptide from ActA.
 (C) Structure of the Homer EVH1 in complex with a 5 residue peptide from mGluR.
 (D) Structure of the RanBP EVH1 domain in complex with an extended, >25 residue polypeptide from Ran. Note that contacts between the EVH1 domain and other parts of Ran are made in the complex.
 Top and bottom images show two views rotated by 90° around a horizontal axis in the plane of the page. Note that in the N-WASP complex, the peptide ligand is recognized in the reverse N- to C-terminal orientation from other EVH1 complexes.

similarity to the interaction of the Ran Binding Protein (RanBP) EVH1 domain with a fragment from the nuclear import protein Ran (Figure 3D). In the crystal structure of the Ran-RanBP complex, a ~25 residue polypeptide sequence from Ran wraps around the entire RanBP EVH1 domain, following the same path as that observed for the WIP peptide when binding the N-WASP EVH1 domain (Vetter et al., 1999). This interaction, however, is only one of several extensive regions of contact between the Ran and RanBP proteins, and it is unknown if this wrapping interaction alone is sufficient for binding, as is the case for the N-WASP/WIP interaction.

In the current NMR structure, the conformation of residues 479–485 (C-terminal end of the WIP peptide) are poorly defined because of a lack of resonance assignments. The difficulty in assigning these residues may be a result of several possibilities: first, the main chain amide protons may have relatively high solvent accessibility and exchange rates; second, the residues may exist in multiple conformations that interconvert within the intermediate exchange regime; and third, the region may be highly mobile. Dynamics of the polypeptide backbone were probed using the ¹⁵N-¹H heteronuclear NOE. For residues 477–480, decreasing NOE values are observed moving from N- to C-terminal, a trend consistent with enhanced mobility for the adjacent unobserved residues (data not shown). Nonetheless, extension of the peptide C terminus beyond residue 480 is energetically important for binding (Figure 1E). We hypothesize that side chain atoms in this region of the peptide make primary contacts with the EVH1 domain, while the main chain atoms may be relatively mobile. As shown in Figure 3A, these residues are most likely

to continue wrapping further around the N-WASP EVH1 domain, along a continued path similar to that observed in the RanBP/Ran interaction.

The extensive interaction interface in the N-WASP/WIP interaction may explain the biochemical behavior of the domain—this exposed, largely hydrophobic binding surface may lead to the poor solubility of the unliganded domain. Association of N-WASP with WIP or a related ligand may be obligatory for proper folding of the protein—consistent with the observation that the N-WASP/WIP interaction appears to be constitutive *in vivo*.

Common Elements of Proline-Rich Peptide Binding

The most N-terminal portion of the WIP polypeptide, which contains the sequence LPPP, binds at the same conserved aromatic surface used by other EVH1 domains for proline peptide binding (Figure 4). As is observed in other EVH1-peptide complexes, this region of the peptide adopts a polyproline II (PPII) helical conformation, a left-handed helix with three residues per turn. Other proline-rich motif binding domains, including SH3 and WW domains, and profilin also recognize their ligands in a PPII conformation. The PPII helix docks against a complementary surface of largely aromatic side chains in a manner very similar to that observed in other EVH1 domains. A universal element of this recognition is a central, conserved tryptophan residue (Trp 54), which forms a ridge over which the PPII helix packs, making favorable van der Waals contact. In addition, the tryptophan indole nitrogen proton forms a hydrogen bond with a carbonyl oxygen of the PPII ligand. Less well conserved but largely hydrophobic residues comprise

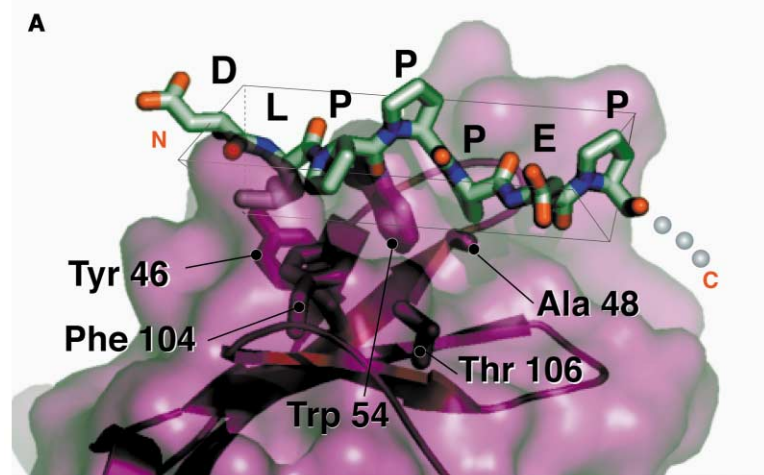
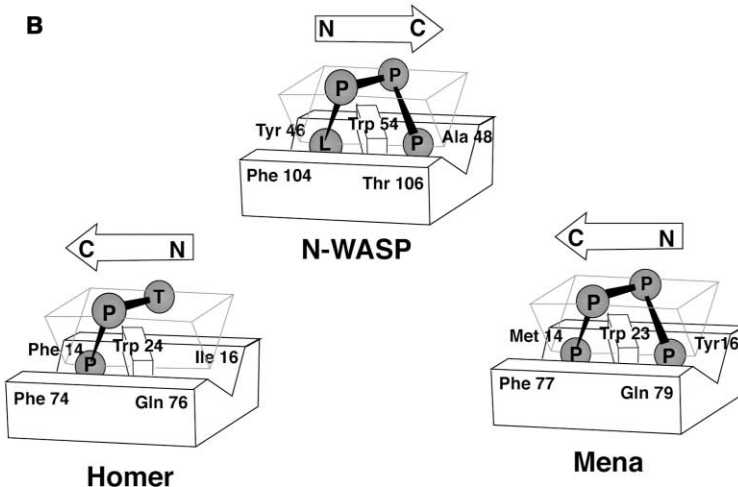


Figure 4. The N-WASP EVH1 Surface Used to Recognize the Proline-Rich Element in the WIP Ligand Is Similar to that Used by Other EVH1 Domains

(A) Close-up view of region of N-WASP EVH1 domain that contacts residues 481–487 of the WIP ligand. The ligand adopts a polyproline II (PPII) helical conformation that docks over Trp 54. The carbonyl oxygen between the apical ligand prolines also makes a hydrogen bond to the Trp nitrogen. Pockets surrounding Trp 54 are made by residues 46 and 104 or 48 and 106.

(B) Corresponding residues in the Homer and Mena EVH1 domains are also used in recognition of the proline-rich peptide ligand. In these structures, however, the PPII helix binds in the opposite N- to C-terminal orientation.



residue binding pockets that flank the central tryptophan.

Two Orientations for EVH1-Peptide Binding

One of the most striking features of this structure is that the WIP polypeptide docks on the EVH1 domain in an N- to C-terminal orientation that is the reverse of that observed in all previous EVH1-peptide complexes (Figures 3 and 4B). Thus, the EVH1 domain, like other proline-rich binding modules (including SH3 and WW domains) and profilin, can bind PPII ligands in two possible orientations. This orientational flexibility, first explored in depth for SH3 domains, is due largely to the 2-fold rotational pseudosymmetry of the PPII structure, both in terms of shape and hydrogen bonding moieties (Lim et al., 1994; Feng et al. 1994). This rotational symmetry allows the relatively isoenergetic docking of the PPII helix in two orientations against a single compatible surface. It is interesting to note that in the RanBP EVH1 structure, the extended peptide from Ran binds in the opposite orientation from that observed in the current structure.

Buried Mutations Linked to Wiskott-Aldrich Syndrome

Because of the extremely high homology between WASP and N-WASP (Figure 2), this EVH1 domain structure and its novel mode of peptide binding provides the first opportunity to accurately interpret missense mutations that result in the disease WAS. WAS is an X-linked recessive disorder that is characterized by thrombocytopenia (platelet deficiency), eczema, and recurrence of bacterial and viral infections. A mild form of the disease is known as X-linked thrombocytopenia (XLT). WAS/XLT-causing missense mutations occur at ~30 residues within the WASP EVH1 domain. For the discussion below we will describe sites of interaction using the residue numbering for N-WASP. However, for clarity and comparison, the corresponding residue number from WASP will also be given in square brackets.

Several of the common WAS-causing mutations map to the hydrophobic core of the EVH1 domain, especially at residues that are absolutely conserved between WASP and N-WASP (Table 2A, Figure 5A). Mutations at buried positions often destabilize a protein and indirectly decrease function. However, it is noteworthy that

Table 2. WAS Missense Mutations Localized to the EVH1 Domain and Their Role in the N-WASP-WIP Complex

Type of Mutation	Position in N-WASP [WASP numbering]	Substitution	Disease Severity	Description of Position	Probable Effect
(A) BURIED	Trp87 [97]	Cys	strong	core	destabilization/conform. change
	His105 [115]	Tyr	strong	core; H bond to Tyr97	destabilization/conform. change
	Phe118 [128]	Ser	strong	core; beneath pept. bind. surf.	destabilization/conform. change
	Ala124 [134]	Thr	strong	core	destabilization/conform. change
	Tyr73 [83]	Cys	mild	core; beneath pept. bind. surf.	destabilization/conform. change ^a
(B) SURFACE	Tyr97 [107]	Cys	mild	core; H bond to His 105	destabilization/conform. change ^a
	Leu31 [39]	Pro	strong	near peptide C term.	disrupt WIP interaction
	Cys63 [73]	Arg	strong	near peptide N term.	disrupt WIP interaction
	Val65 [75]	Met	strong	near peptide C term.	disrupt WIP interaction
	Ser72 [82]	Phe	strong	near peptide C term. (NOE)	disrupt WIP interaction
	Arg76 [86]	Cys, His, Leu, Pro	strong	near peptide C term.	disrupt WIP interaction ^a
	Arg101 [111]	Pro	strong	near peptide C term. (NOE)	disrupt WIP interaction
	Ala115 [Gly125]	Arg	strong	near peptide N term. (NOE)	disrupt WIP interaction
	Glu123 [133]	Lys	strong	away from peptide	structural salt bridge?
	Thr37 [45]	Met	mild (XLT)	near peptide C term.	disrupt WIP interaction
	Gln44 [52]	His	mild (XLT)	near peptide N term.	disrupt WIP interaction
	Lys33 [Arg41]	Gly	mild	near peptide C term.	disrupt WIP interaction
	Ser39 [47]	Asp	mild	near peptide C term.	disrupt WIP interaction
	Ser40 [48]	Ile	mild	near peptide C term.	disrupt WIP interaction
	Ala48 [56]	Val	mild	near peptide N term. (NOE)	disrupt WIP interaction
	Phe74 [84]	Leu	mild	near peptide C term.	disrupt WIP interaction
	Gln89 [99]	Arg	mild	near peptide C term. (NOE)	disrupt WIP interaction
	Gly109 [119]	Glu	mild	near peptide N term. (NOE)	disrupt WIP interaction
	Glu121 [131]	Lys	mild	salt bridge with Lys125	destabilization/conform. change
	Arg128 [138]	Pro	strong	H bond to Ser99	destabilization/conform. change

Data compiled from WASP database (<http://www.tmd.ac.jp/med/ped/WASPbase.html>)

“NOE” indicates observed NOE contact between WIP peptide and this residue.

^aMutation experimentally observed to disrupt WASP-WIP interaction by yeast two-hybrid assay (Stewart et al., 1999).

many of these buried mutations cluster into a single packing unit (Trp87 [97], Tyr97 [107], His105 [115], Phe118 [128], and Ala124 [134]) that includes a buried hydrogen bond between residues Tyr97 [107] and His105 [115]. Even fairly subtle mutations at these positions (i.e., Tyr97 [107]-Cys, His105 [115]-Tyr, Ala124 [134]-Thr), which maintain hydrophobicity and thus might not be expected to be very destabilizing, result in the disease. Interestingly, this packing unit lies directly beneath the proline-rich peptide binding surface. In fact, one of these residues, His105 [115], is the covalent neighbor of two residues that directly contact this segment of the WIP ligand (Phe104 [114], Thr106 [116]). Thus, it seems possible that subtle mutations in this packing unit perturb the precise stereochemistry of the proline-rich peptide binding surface and thereby impair WIP binding. This hypothesis is consistent with several previous findings: first, the Tyr97 [107]-Cys and Ala124 [134]-Thr mutations were found to impair interaction with WIP in an *in vitro* yeast two-hybrid binding assay (Stewart et al., 1999); and second, studies of patient samples reveal no significant decrease of endogenous expression levels of the WASP protein in a patient bearing a mutation at Tyr97 [107].

Surface Mutations Linked to Wiskott-Aldrich Syndrome

Approximately 20 of the reported WAS-causing mutations map to the EVH1 domain surface (Table 2B, Figure 5B). Oddly, there are no naturally occurring mutations at the proline-rich peptide binding surface (although mu-

tation of Trp54 has been shown to disrupt proper localization to vaccinia virus (Moreau et al., 2000). In fact, the most dramatic hotspot of disease mutations is on the face of the EVH1 domain directly opposite the proline-rich peptide binding surface (Beneken et al., 2000). For example, the most frequent mutated residue resulting in a severe disease phenotype is Arg76 [86]. Every possible single base change missense mutation (Cys, His, Leu, Pro) has been found in the WAS patient population (Table 2B). Mutations are also found at other surface residues that flank Arg76 [86], including Leu31 [39], Thr37 [45], Ser40 [Thr48], Cys63 [73], and Phe74 [84]. Given the distance of this mutational hotspot from the canonical peptide binding site identified in previously characterized EVH1 domain complexes, it has been difficult to reconcile how these mutations in WASP might disrupt EVH1 domain interactions and function (Beneken et al., 2000).

In the context of this new structure, however, we now know that the WIP ligand wraps around the N-WASP EVH1 domain, extending from the canonical proline-rich peptide-docking site all the way to mutational hotspot surrounding Arg76 [86]. Contacts made in this region are therefore likely to be critical for WIP binding. Unfortunately, because of a lack of assignments, we do not know the precise conformation of the last seven residues of the WIP polypeptide and exactly how these residues interact with the hotspot centered around Arg76 [86]. However, these seven residues are required for binding and therefore must be involved in energetically important interactions.

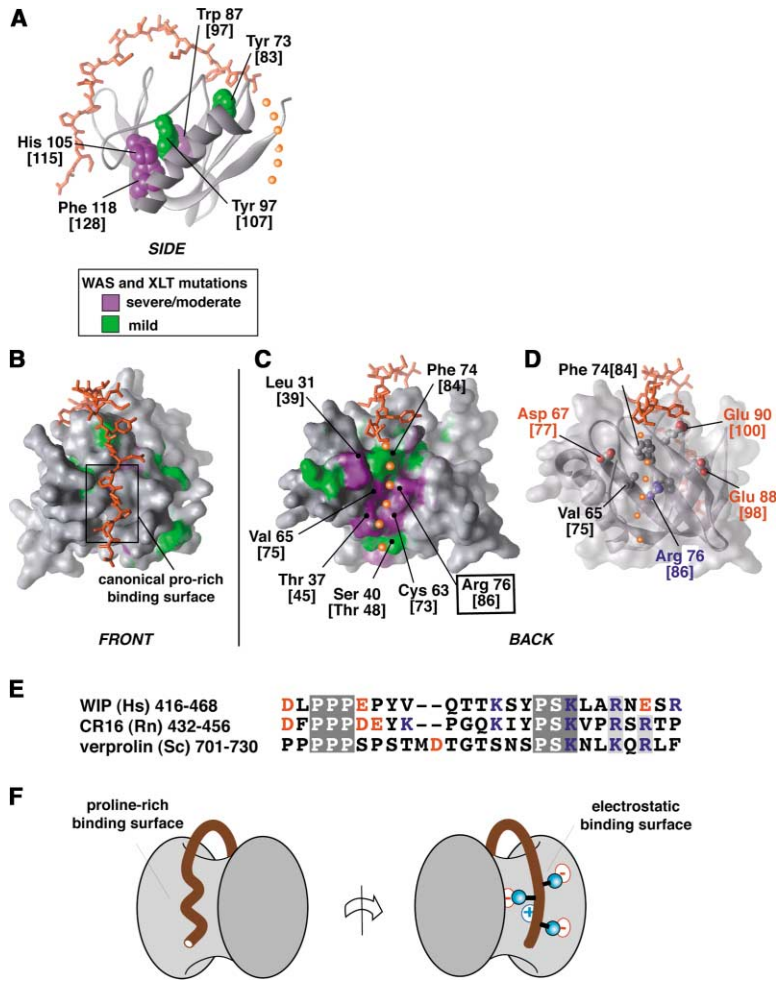


Figure 5. Structural Basis of Mutations that Cause the Disorder WAS

(A) Residues in the core of the N-WASP EVH1 domain that when mutated lead to WAS are shown in space-filling depiction. Severe/moderate mutations are colored in lavender; mild mutations are colored in green. Residue numbering is that of N-WASP, with the corresponding numbering from WASP given in square brackets. Peptide is colored orange, with the postulated path of the peptide C terminus indicated by small orange spheres.

(B) Front face of N-WASP EVH1 domain indicating surface mutations associated with WAS. Residues are colored as above.

(C) Back face of N-WASP EVH1 domain, indicating surface mutations associated with WAS. Molecular has been rotated 180° from the view in (B).

(D) Transparent surface view identical to that in (C) reveals a conserved network of charged residues, centered around Arg76 [86] (see Figure 2 for conservation).

(E) Alignment of WIP homologs in the WASP binding peptide reveals two regions of high conservation, including the C-terminal PSKxxR/K motif that is likely to dock at the surface shown in (D). Charged residues are colored in red (negative) or blue (positive).

(F) Cartoon of how the extended WIP peptide and its homologs may wrap around the N-WASP EVH1 domain to contact two distant but energetically important binding surfaces.

Based on the evidence given below, we postulate that the C-terminal end of the WIP peptide binds at this mutational hotspot and participates in an energetically critical network of electrostatic interactions. First, the proposed binding path for the remaining portions of the peptide correlates exactly with the binding groove utilized by the RanBP EVH1 domain to recognize one terminus of the Ran peptide (see Figure 3D). Second, mutation of the central Arg76 [86] to His has been shown to impair interaction with WIP in an in vitro yeast two-hybrid assay (Stewart et al., 1999). Third, Arg76 [86] is the central residue in a conserved electrostatic network presented on this surface of the EVH1 domain (Figure 5D). Surrounding Arg76 [86] are a ring of acidic residues, Asp67 [77], Glu88 [98], and Glu90 [100] (Figure 5D), all of which are conserved from human WASP/N-WASP to the yeast ortholog, Bee1p (see Figure 2). In the current structure, Arg76 [86] is very well ordered for an arginine residue—several interresidue NOEs are observed for the Arg side chain, and its epsilon NH proton exchanges very slowly. This observation is consistent with Arg76 [86] playing a central role in coordinating and orienting this otherwise repulsive network of surrounding acidic residues. Fourth, the C terminus of the WIP peptide contains a cluster of basic residues that is very well

conserved in all WIP homologs, including mouse WIP, human CR16, and yeast verprolin—all of which have been shown to interact with WASP or WASP homologs (Figure 5E). This cluster of basic residues is within the conserved motif: P-S-K-x-x-R/K-x₍₁₋₃₎-R. In summary, we therefore propose a model in which the conserved basic motif found at the C terminus of the WIP ligand specifically interacts with a complementary network of conserved acidic residues that are properly positioned by the central Arg76 [86] residue (Figure 5F). Such an interaction may have a fairly high degree of mobility, consistent with the difficulty in observing assignable resonances, despite its apparent energetic importance.

Overall, this structure is therefore consistent with a simple model for the cause of WAS: the major defect in these diverse WAS missense mutations is likely to be disruption of the interaction with WIP. Disruption of this interaction may prevent proper subcellular targeting of WASP. The reason that mutations are found at sites widely spread over the EVH1 domain surface, well beyond the canonical EVH1 peptide binding surface, is because this EVH1 domain utilizes a novel mode of interaction—the WIP ligand wraps around almost two-thirds of the entire circumference of the EVH1 domain, contacting many distant surfaces.

Conclusions

This structure of the N-WASP EVH1 domain in complex with a peptide ligand from WIP reveals a novel mechanism of peptide recognition by EVH1 domains and highlights the versatility of EVH1 domains as a recognition platform. While the majority of EVH1 domains and other similar protein-protein modules bind short 6–12 residue motifs, the N-WASP EVH1 domain binds a single long 25 residue motif. Comparison of the WIP ligand and its homologs from different species suggest that there are two conserved submotifs that are recognized: the N-terminal PPP submotif, similar to other EVH1 ligands, and the C-terminal PSKxxR submotif. These two submotifs interact on opposite faces of the EVH1 domain, leading to this very extensive wrapping mechanism of recognition (Figures 5E and 5F). The extensive binding surface employed provides an explanation for the spatially dispersed set of WAS-causing mutants that map to the EVH1 domain.

This interaction represents a novel or hybrid class of protein-protein interactions. Most protein-protein interactions are divided into two major classes: (1) interactions that involve the docking of two large folded protein surfaces, and (2) interactions that involve the docking of a short, largely linear peptide epitope on a protein surface (Stanfield and Wilson, 1995). Like the second class of interactions, the N-WASP EVH1-WIP peptide interaction involves recognition of a linear epitope. However, because the epitope is extremely long, the contact area involved is as large as that observed in the first class of interactions. It will be interesting to see if other EVH1 domains also have the ability to recognize longer peptides with higher specificity by utilizing more of their surface binding potential. It is also possible that in some cases EVH1 domains may be able to use their extensive binding surfaces to simultaneously interact with two or more ligands, recognizing short, proline-rich peptides with the canonical binding surface and recognizing other yet unidentified ligands at remaining portions of the domain surface.

Experimental Procedures

Lipid Vesicle Binding Assays

Cosedimentation lipid vesicle binding assays were performed as described by Kavran et al. (1998). Specifically, 3 μ M protein and vesicles (\sim 20 μ M PIP₂) were mixed in 20 mM HEPES (pH 7.0), 100 mM NaCl, 1 mM DTT (total assay volume 85 μ l), incubated at 25°C for 5 min, and centrifuged at 100,000 \times g for 15 min. The vesicles comprised PC:PS:PIP₂ at ratios of 48:48:2. Apparent concentrations of PIP₂ were calculated as 50% of total. The vesicle pellet was washed with 1000 μ l of buffer three times and suspended in a volume of buffer equal to the supernatant. Bound (pellet) and unbound proteins (supernatant) were identified by SDS-PAGE. This assay can detect binding of the PLC- δ PH domain, which has an affinity for PIP₂ of $K_d = 2 \mu$ M.

Far-Western Protein Binding Assays

Assays were performed as described (Prehoda et al., 1999). Putative EVH1 peptide ligands were generated as fusions to glutathione S-transferase (GST), electrophoresed on a 10%–20% SDS-PAGE gel, and transferred to nitrocellulose by electroblotting, and the blot was blocked for 1 hr at 4°C in Superblock (Pierce). Biotinylated EVH1 domains were produced as fusions to a naturally biotinylated *E. coli* protein using the PIN-POINT system (Promega). The soni-

cated and centrifuged lysate was used directly as probe, after estimating fusion protein concentration by SDS-PAGE. Washing and chemiluminescence detection was performed as described (Prehoda et al., 1999).

Protein Labeling and Purification

The WIP-EVH1 sequence (residues 461–485 of human WIP and residues 26–147 of rat N-WASP, linked by the intervening sequence GSGSG) was ligated into the pBH4 expression vector, which contains a His6-tag followed by a Tobacco Etch Virus (TEV) protease cleavage site. For uniform labeling with ¹⁵N and ¹³C, BL21(DE3) cells freshly transformed with the WIP-EVH1 expression plasmid were grown in M9 minimal media containing [¹³C]glucose (2 g/l) and [¹⁵N]ammonium chloride (1 g/l) as the respective sole carbon and nitrogen sources. Expression was induced by the addition of IPTG to a final concentration of 1 mM. After expression for 3 hr, the cells were harvested by centrifugation, resuspended in Lysis Buffer (50 mM PO₄, 300 mM NaCl, 10 mM imidazole [pH 8.0]), disrupted by sonication, and centrifuged, and the soluble fraction bound in batch to Ni-NTA agarose. After extensive washing with lysis buffer, bound protein was eluted with lysis buffer + 300 mM imidazole. The His6-tag was removed by incubation with TEV protease for 2 hr at room temperature. Cleaved WIP-EVH1 protein was further purified on a ResourceS (Pharmacia) column at pH 7.5 with a 1–500 mM NaCl gradient. Pure protein was pooled and concentrated to \sim 1 mM. Protein size was confirmed by mass spectroscopy before and after NMR data collection.

A cleavable version of the linked WIP-EVH1 protein was generated as described above, but with an intervening linker sequence GGLVPRGSGG (underlined sequence is thrombin cleavage site). ¹³C/¹⁵N-labeled protein was prepared as described above and cleaved at a concentration of 0.5 mM by adding 50 nM of bovine thrombin (Sigma). Cleavage was complete in 1 hr as monitored by SDS-PAGE.

NMR Spectroscopy

NMR experiments were carried out on Bruker DRX600 spectrometers, either at the Medical College of Wisconsin (with triple-resonance Z-axis gradient CryoProbe[®]) or at the National Magnetic Resonance Facility at Madison (with conventional probe). Samples contained \sim 1 mM WIP-EVH1 protein in 90% H₂O/10% D₂O with 20 mM sodium phosphate (pH 7.0), 20 mM sodium chloride, 1 mM dithiothreitol, and 0.05% sodium azide. Resonance assignments and distance constraints were derived from the following experiments: 3D ¹⁵N NOESY-HSQC (Talluri and Wagner, 1996), 3D ¹⁵N SE TOCSY-HSQC (Zhang et al., 1994), 3D HCCH-TOCSY (Kay et al., 1993), 3D SE CCONH (Grzesiek et al., 1993), 3D SE HNCA (Grzesiek and Bax, 1992; Kay et al., 1994), 3D SE HNCOC (Grzesiek and Bax, 1992), 3D SE HNCO (Grzesiek and Bax, 1992; Muhandiram and Kay, 1994), 3D ¹³C SE NOESY-HSQC (one each for the aromatic and aliphatic ¹³C regions) (Kay et al., 1993), and ¹³C constant-time SE HSQC (Santoro and King, 1992). NOESY mixing times were 80 ms. Isotropic mixing periods were 22 ms (CCONH) and 60 ms (¹⁵N TOCSY-HSQC). Heteronuclear NOEs were measured from an interleaved pair of 2D ¹⁵N-¹H gradient sensitivity enhanced correlation spectra (Farrow et al., 1994) recorded with and without a 3.5 s proton saturation period using a total recycle delay of 5.5 s. Data were processed using NMRPipe (Delaglio et al., 1995) and analyzed using XEASY (Bartels et al., 1995). Chemical shifts were referenced to 2,2-dimethylsilapentane-5-sulfonic acid (DSS) directly for ¹H and indirectly for ¹⁵N and ¹³C (Markley et al., 1998). The CSI program was used for determining the secondary structure from the chemical shift index (Wishart and Sykes, 1994; Wishart et al., 1992). For the thrombin-cleaved protein, resonance assignments and NOE patterns were determined for the cleaved WIP-EVH1 complex using 3D SE HNCA, 3D CCONH, 3D ¹⁵N NOESY-HSQC, and 3D ¹³C NOESY-HSQC spectra, under the same conditions. No significant chemical shift differences were observed apart from residues of the linker that differ in the two constructs (see Supplemental Figure S1 at <http://www.cell.com/cgi/content/full/111/4/565/DC1>), and both samples displayed the same pattern of WIP-EVH1 NOEs.

Structure Calculation and Analysis

Structures were iteratively refined using the simulated annealing protocol (10,000 steps total) of the torsion angle dynamics program DYANA (Güntert et al., 1997). NOE peak intensities were converted into upper distance bounds with the CALIBA function of DYANA. A total of 143 ϕ and ψ dihedral angle constraints were generated from $^1\text{H}^\alpha$, $^{13}\text{C}^\alpha$, $^{13}\text{C}^\beta$, $^{13}\text{C}^\gamma$, and ^{15}N secondary shifts using TALOS (Cornilescu et al., 1999). Of the final 50 structures calculated, the 20 conformers with the lowest target function values were selected for analysis. The mean structure, calculated from this ensemble of 20 structures in MOLMOL (Koradi et al., 1996), was minimized in DYANA using 8000 steps of conjugate gradient minimization. Coordinates (minimized average structure and final 20 structures) have been deposited in the RCSB database (accession code 1MKE). Residues in the PDB file are numbered consecutively with the following residue number translation: PDB(1–25) = WIP(461–485); PDB(26–30) = GSGSG linker; PDB(31–144) = N-WASP(26–139) (note: residues 140–147 of N-WASP were not observed by NMR and are not included in the PDB file).

Received: April 17, 2002

Revised: September 4, 2002

References

- Ball, L.J., Kuhne, R., Hoffmann, B., Hafner, A., Schmieder, P., Volkmer-Engert, R., Hof, M., Wahl, M., Schneider-Mergener, J., Walter, U., et al. (2000). Dual epitope recognition by the VASP EVH1 domain modulates polyproline ligand specificity and binding affinity. *EMBO J.* **19**, 4903–4914.
- Bartels, C., Xia, T.-H., Billeter, M., Güntert, P., and Wüthrich, K. (1995). The program XEASY for computer-supported NMR spectral analysis of biological macromolecules. *J. Biomol. NMR* **5**, 1–10.
- Barzik, M., Carl, U.D., Schubert, W.D., Frank, R., Wehland, J., and Heinz, D.W. (2001). The N-terminal domain of Homer/Ves1 is a new class II EVH1 domain. *J. Mol. Biol.* **309**, 155–169.
- Beneken, J., Tu, J.C., Xiao, B., Nuriya, M., Yuan, J.P., Worley, P.F., and Leahy, D.J. (2000). Structure of the Homer EVH1 domain-peptide complex reveals a new twist in polyproline recognition. *Neuron* **26**, 143–154.
- Callebaut, I., Cossart, P., and Dehoux, P. (1998). EVH1/WH1 domains of VASP and WASP proteins belong to a large family including Ran-binding domains of the RanBP1 family. *FEBS Lett.* **441**, 181–185.
- Cannon, J.L., Labno, C.M., Bosco, G., Seth, A., McGavin, M.H., Siminovitch, K.A., Rosen, M.K., and Burkhardt, J.K. (2001). Wasp recruitment to the T cell:APC contact site occurs independently of Cdc42 activation. *Immunity* **15**, 249–259.
- Carl, U.D., Pollmann, M., Orr, E., Gertler, F.B., Chakraborty, T., and Wehland, J. (1999). Aromatic and basic residues within the EVH1 domain of VASP specify its interaction with proline-rich ligands. *Curr. Biol.* **9**, 715–718.
- Carlier, M.F., Ducruix, A., and Pantaloni, D. (1999). Signalling to actin: the Cdc42-N-WASP-Arp2/3 connection. *Chem. Biol.* **6**, R235–R240.
- Carlier, M.F., Nioche, P., Broutin-L'Hermite, I., Boujemaa, R., Le Clainche, C., Egile, C., Garbay, C., Ducruix, A., Sansonetti, P., and Pantaloni, D. (2000). GRB2 links signaling to actin assembly by enhancing interaction of neural Wiskott-Aldrich syndrome protein (N-WASP) with actin-related protein (ARP2/3) complex. *J. Biol. Chem.* **275**, 21946–21952.
- Coppolino, M.G., Krause, M., Hagendorff, P., Monner, D.A., Trimble, W., Grinstein, S., Wehland, J., and Sechi, A.S. (2001). Evidence for a molecular complex consisting of Fyb/SLAP, SLP-76, Nck, VASP and WASP that links the actin cytoskeleton to Fc γ receptor signalling during phagocytosis. *J. Cell Sci.* **114**, 4307–4318.
- Cornilescu, G., Delaglio, F., and Bax, A. (1999). Protein backbone angle restraints from searching a database for chemical shift and sequence homology. *J. Biomol. NMR* **13**, 289–302.
- Delaglio, F., Grzesiek, S., Vuister, G.W., Zhu, G., Pfeifer, J., and Bax, A. (1995). NMRPipe: a multidimensional spectral processing system based on UNIX pipes. *J. Biomol. NMR* **6**, 277–293.
- Derry, J.M., Ochs, H.D., and Francke, U. (1994). Isolation of a novel gene mutated in Wiskott-Aldrich syndrome. *Cell* **78**, 635–644.
- Derry, J.M., Kerns, J.A., Weinberg, K.I., Ochs, H.D., Volpini, V., Estivill, X., Walker, A.P., and Francke, U. (1995). WASP gene mutations in Wiskott-Aldrich syndrome and X-linked thrombocytopenia. *Hum. Mol. Genet.* **4**, 1127–1135.
- El-Hakeh, J., Rosenzweig, S., Oleastro, M., Basack, N., Berozdnic, L., Molina, F., Rivas, E.M., Zelazko, M., and Danielian, S. (2002). Wiskott-Aldrich syndrome in Argentina: 17 unique, including nine novel, mutations. *Hum. Mutat.* **19**, 186–187.
- Farrow, N.A., Muhandiram, R., Singer, A.U., Pascal, S.M., Kay, C.M., Gish, G., Shoelson, S.E., Pawson, T., Forman-Kay, J.D., and Kay, L.E. (1994). Backbone dynamics of a free and a phosphopeptide-complexed src homology 2 domain studied by ^{15}N NMR relaxation. *Biochemistry* **33**, 5984–6003.
- Fedorov, A.A., Fedorov, E., Gertler, F., and Almo, S.C. (1999). Structure of EVH1, a novel proline-rich ligand-binding module involved in cytoskeletal dynamics and neural function. *Nat. Struct. Biol.* **6**, 661–665.
- Feng, S., Chen, J.K., Yu, H., Simon, J.A., and Schreiber, S.L. (1994). Two binding orientations for peptides to the Src SH3 domain: development of a general model for SH3-ligand interactions. *Science* **266**, 1241–1247.
- Gertler, F.B., Niebuhr, K., Reinhard, M., Wehland, J., and Soriano, P. (1996). Mena, a relative of VASP and Drosophila Enabled, is implicated in the control of microfilament dynamics. *Cell* **87**, 227–239.
- Greer, W.L., Shehabeldin, A., Schulman, J., Junker, A., and Siminovitch, K.A. (1996). Identification of WASP mutations, mutation hot-spots and genotype-phenotype disparities in 24 patients with the Wiskott-Aldrich syndrome. *Hum. Genet.* **98**, 685–690.
- Grzesiek, S., and Bax, A. (1992). Improved 3D triple-resonance NMR techniques applied to a 31 kDa protein. *J. Magn. Reson.* **96**, 432–440.
- Grzesiek, S., Anglister, J., and Bax, A. (1993). Correlation of backbone amide and aliphatic side-chain resonances in $^{13}\text{C}/^{15}\text{N}$ -enriched proteins by isotropic mixing of ^{13}C magnetization. *J. Magn. Reson.* **101**, 114–119.
- Güntert, P., Mumenthaler, C., and Wüthrich, K. (1997). Torsion angle dynamics for NMR structure calculation with the new program DYANA. *J. Mol. Biol.* **273**, 283–298.
- Higgs, H.N., and Pollard, T.D. (2000). Activation by Cdc42 and PIP(2) of Wiskott-Aldrich syndrome protein (WASP) stimulates actin nucleation by Arp2/3 complex. *J. Cell Biol.* **150**, 1311–1320.
- Higgs, H.N., and Pollard, T.D. (2001). Regulation of actin filament network formation through ARP2/3 complex: activation by a diverse array of proteins. *Annu. Rev. Biochem.* **70**, 649–676.
- Ho, H.Y., Rohatgi, R., Ma, L., and Kirschner, M.W. (2001). CR16 forms a complex with N-WASP in brain and is a novel member of a conserved proline-rich actin-binding protein family. *Proc. Natl. Acad. Sci. USA* **98**, 11306–11311.
- Imai, K., Nonoyama, S., Miki, H., Morio, T., Fukami, K., Zhu, Q., Aruffo, A., Ochs, H.D., Yata, J., and Takenawa, T. (1999). The pleckstrin homology domain of the Wiskott-Aldrich syndrome protein is involved in the organization of actin cytoskeleton. *Clin. Immunol.* **92**, 128–137.
- Insall, R., and Machesky, L. (1999). PH domains in WASP—a bug in the system? Wiskott-Aldrich syndrome protein. *Trends Cell Biol.* **9**, 211–212.
- Kavran, J.M., Klein, D.E., Lee, A., Falasca, M., Isakoff, S.J., Skolnik, E.Y., and Lemmon, M.A. (1998). Specificity and promiscuity in phosphoinositide binding by pleckstrin homology domains. *J. Biol. Chem.* **273**, 30497–30508.
- Kay, L.E., Xu, G.-Y., Singer, A.U., Muhandiram, D.R., and Forman-Kay, J.D. (1993). A gradient-enhanced HCCH-TOCSY experiment for recording sidechain ^1H and ^{13}C correlations in H $_2\text{O}$ samples of proteins. *J. Magn. Reson.* **101**, 333–337.
- Kay, L.E., Xu, G.Y., and Yamazaki, T. (1994). Enhanced-sensitivity triple-resonance spectroscopy with minimal H $_2\text{O}$ saturation. *J. Magn. Reson.* **109**, 129–133.
- Kim, A.S., Kakalis, L.T., Abdul-Manan, N., Liu, G.A., and Rosen, M.K.

- (2000). Autoinhibition and activation mechanisms of the Wiskott-Aldrich syndrome protein. *Nature* 404, 151–158.
- Kolluri, R., Shehabeldin, A., Peacocke, M., Lamhonwah, A.M., Teichert-Kuliszewska, K., Weissman, S.M., and Siminovich, K.A. (1995). Identification of WASP mutations in patients with Wiskott-Aldrich syndrome and isolated thrombocytopenia reveals allelic heterogeneity at the WAS locus. *Hum. Mol. Genet.* 4, 1119–1126.
- Koradi, R., Billeter, M., and Wüthrich, K. (1996). MOLMOL: a program for display and analysis of macromolecular structures. *J. Mol. Graph.* 14, 51–55.
- Leverrier, Y., Lorenzi, R., Blundell, M.P., Brickell, P., Kinnon, C., Ridley, A.J., and Thrasher, A.J. (2001). Cutting edge: the Wiskott-Aldrich syndrome protein is required for efficient phagocytosis of apoptotic cells. *J. Immunol.* 166, 4831–4834.
- Lim, W.A., Richards, F.M., and Fox, R.O. (1994). Structural determinants of peptide-binding orientation and of sequence specificity in SH3 domains. *Nature* 372, 375–379.
- Machesky, L.M., and Insall, R.H. (1998). Scar1 and the related Wiskott-Aldrich syndrome protein, WASP, regulate the actin cytoskeleton through the Arp2/3 complex. *Curr. Biol.* 8, 1347–1356.
- Markley, J.L., Bax, A., Arata, Y., Hilbers, C.W., Kaptein, R., Sykes, B.D., Wright, P.E., and Wüthrich, K. (1998). Recommendations for the presentation of NMR structures of proteins and nucleic acids. *Pure Appl. Chem.* 70, 117–142.
- Martinez-Quiles, N., Rohatgi, R., Anton, I.M., Medina, M., Saville, S.P., Miki, H., Yamaguchi, H., Takenawa, T., Hartwig, J.H., Geha, R.S., and Ramesh, N. (2001). WIP regulates N-WASP-mediated actin polymerization and filopodium formation. *Nat. Cell Biol.* 3, 484–491.
- Miki, H., Miura, K., and Takenawa, T. (1996). N-WASP, a novel actin-depolymerizing protein, regulates the cortical cytoskeletal rearrangement in a PIP2-dependent manner downstream of tyrosine kinases. *EMBO J.* 15, 5326–5335.
- Miki, H., Sasaki, T., Takai, Y., and Takenawa, T. (1998). Induction of filopodium formation by a WASP-related actin-depolymerizing protein N-WASP. *Nature* 391, 93–96.
- Millard, T.H., and Machesky, L.M. (2001). The Wiskott-Aldrich syndrome protein (WASP) family. *Trends Biochem. Sci.* 26, 198–199.
- Moreau, V., Frischknecht, F., Reckmann, I., Vincentelli, R., Rabut, G., Stewart, D., and Way, M. (2000). A complex of N-WASP and WIP integrates signalling cascades that lead to actin polymerization. *Nat. Cell Biol.* 2, 441–448.
- Muhandiram, D.R., and Kay, L.E. (1994). Gradient-enhanced triple-resonance three-dimensional NMR experiments with improved sensitivity. *J. Magn. Reson.* 103, 203–216.
- Naqvi, S.N., Zahn, R., Mitchell, D.A., Stevenson, B.J., and Munn, A.L. (1998). The WASP homologue Las17p functions with the WIP homologue End5p/verprolin and is essential for endocytosis in yeast. *Curr. Biol.* 8, 959–962.
- Niebuhr, K., Ebel, F., Frank, R., Reinhard, M., Domann, E., Carl, U.D., Walter, U., Gertler, F.B., Wehland, J., and Chakraborty, T. (1997). A novel proline-rich motif present in ActA of *Listeria monocytogenes* and cytoskeletal proteins is the ligand for the EVH1 domain, a protein module present in the Ena/VASP family. *EMBO J.* 16, 5433–5444.
- Pollard, T.D., Blanchoin, L., and Mullins, R.D. (2000). Molecular mechanisms controlling actin filament dynamics in nonmuscle cells. *Annu. Rev. Biophys. Biomol. Struct.* 29, 545–576.
- Prehoda, K.E., Lee, D.J., and Lim, W.A. (1999). Structure of the enabled/VASP homology 1 domain-peptide complex: a key component in the spatial control of actin assembly. *Cell* 97, 471–480.
- Prehoda, K.E., Scott, J.A., Mullins, R.D., and Lim, W.A. (2000). Integration of multiple signals through cooperative regulation of the N-WASP-Arp2/3 complex. *Science* 290, 801–806.
- Ramesh, N., Anton, I.M., Hartwig, J.H., and Geha, R.S. (1997). WIP, a protein associated with wiskott-aldrich syndrome protein, induces actin polymerization and redistribution in lymphoid cells. *Proc. Natl. Acad. Sci. USA* 94, 14671–14676.
- Rebecchi, M.J., and Scarlata, S. (1998). Pleckstrin homology domains: a common fold with diverse functions. *Annu. Rev. Biophys. Biomol. Struct.* 27, 503–528.
- Renfranz, P.J., and Beckerle, M.C. (2002). Doing (F/L)PPPPs: EVH1 domains and their proline-rich partners in cell polarity and migration. *Curr. Opin. Cell Biol.* 14, 88–103.
- Rohatgi, R., Ma, L., Miki, H., Lopez, M., Kirchhausen, T., Takenawa, T., and Kirschner, M.W. (1999). The interaction between N-WASP and the Arp2/3 complex links Cdc42-dependent signals to actin assembly. *Cell* 97, 221–231.
- Rohatgi, R., Ho, H.Y., and Kirschner, M.W. (2000). Mechanism of N-WASP activation by CDC42 and phosphatidylinositol 4, 5-bisphosphate. *J. Cell Biol.* 150, 1299–1310.
- Rohatgi, R., Nollau, P., Ho, H.Y., Kirschner, M.W., and Mayer, B.J. (2001). Nck and phosphatidylinositol 4,5-bisphosphate synergistically activate actin polymerization through the N-WASP-Arp2/3 pathway. *J. Biol. Chem.* 276, 26448–26452.
- Santoro, J., and King, G.C. (1992). A constant-time 2D overbroadening experiment for inverse correlation of isotopically enriched species. *J. Magn. Reson.* 97, 202–207.
- Savoy, D.N., Billadeau, D.D., and Leibson, P.J. (2000). Cutting edge: WIP, a binding partner for Wiskott-Aldrich syndrome protein, cooperates with Vav in the regulation of T cell activation. *J. Immunol.* 164, 2866–2870.
- Snapper, S.B., and Rosen, F.S. (1999). The Wiskott-Aldrich syndrome protein (WASP): roles in signaling and cytoskeletal organization. *Annu. Rev. Immunol.* 17, 905–929.
- Snapper, S.B., Rosen, F.S., Mizoguchi, E., Cohen, P., Khan, W., Liu, C.H., Hagemann, T.L., Kwan, S.P., Ferrini, R., Davidson, L., et al. (1998). Wiskott-Aldrich syndrome protein-deficient mice reveal a role for WASP in T but not B cell activation. *Immunity* 9, 81–91.
- Snapper, S.B., Takeshima, F., Anton, I., Liu, C.H., Thomas, S.M., Nguyen, D., Dudley, D., Fraser, H., Purich, D., Lopez-Illasaca, M., et al. (2001). N-WASP deficiency reveals distinct pathways for cell surface projections and microbial actin-based motility. *Nat. Cell Biol.* 3, 897–904.
- Stanfield, R.L., and Wilson, I.A. (1995). Protein-peptide interactions. *Curr. Opin. Struct. Biol.* 5, 103–113.
- Stewart, D.M., Tian, L., and Nelson, D.L. (1999). Mutations that cause the Wiskott-Aldrich syndrome impair the interaction of Wiskott-Aldrich syndrome protein (WASP) with WASP interacting protein. *J. Immunol.* 162, 5019–5024.
- Suzuki, T., Miki, H., Takenawa, T., and Sasakawa, C. (1998). Neural Wiskott-Aldrich syndrome protein is implicated in the actin-based motility of *Shigella flexneri*. *EMBO J.* 17, 2767–2776.
- Symons, M., Derry, J.M., Karlak, B., Jiang, S., Lemahieu, V., McCormick, F., Francke, U., and Abo, A. (1996). Wiskott-Aldrich syndrome protein, a novel effector for the GTPase CDC42Hs, is implicated in actin polymerization. *Cell* 84, 723–734.
- Talluri, S., and Wagner, G. (1996). An optimized 3D NOESY-HSQC. *J. Magn. Reson. B* 112, 200–205.
- Vetter, I.R., Nowak, C., Nishimoto, T., Kuhlmann, J., and Wittinghofer, A. (1999). Structure of a Ran-binding domain complexed with Ran bound to a GTP analogue: implications for nuclear transport. *Nature* 398, 39–46.
- Villa, A., Notarangelo, L., Macchi, P., Mantuano, E., Cavagni, G., Brugnoli, D., Strina, D., Patrosso, M.C., Ramenghi, U., Sacco, M.G., et al. (1995). X-linked thrombocytopenia and Wiskott-Aldrich syndrome are allelic diseases with mutations in the WASP gene. *Nat. Genet.* 9, 414–417.
- Wishart, D.S., and Sykes, B.D. (1994). The 13C chemical shift index: a simple method for the identification of protein secondary structure using 13C chemical shift data. *J. Biomol. NMR* 4, 171–180.
- Wishart, D.S., Sykes, B.D., and Richards, F.M. (1992). The chemical shift index: a fast and simple method for the assignment of protein secondary structure through NMR spectroscopy. *Biochemistry* 31, 1647–1651.

Zhang, O., Kay, L.E., Olivier, J.P., and Forman-Kay, J.D. (1994). Backbone ^1H and ^{15}N resonance assignments of the N-terminal SH3 domain of drk in folded and unfolded states using enhanced-sensitivity pulsed field gradient NMR techniques. *J. Biomol. NMR* **4**, 845–858.

Zhu, Q., Watanabe, C., Liu, T., Hollenbaugh, D., Blaese, R.M., Kanner, S.B., Aruffo, A., and Ochs, H.D. (1997). Wiskott-Aldrich syndrome/X-linked thrombocytopenia: WASP gene mutations, protein expression, and phenotype. *Blood* **90**, 2680–2689.

Zicha, D., Allen, W.E., Brickell, P.M., Kinnon, C., Dunn, G.A., Jones, G.E., and Thrasher, A.J. (1998). Chemotaxis of macrophages is abolished in the Wiskott-Aldrich syndrome. *Br. J. Haematol.* **101**, 659–665.